the FEBS Journal

The endogenous retinoid metabolite *S*-4-oxo-9-*cis*-13,14-dihydro-retinoic acid activates retinoic acid receptor signalling both *in vitro* and *in vivo*

Jan P. Schuchardt[1], David Wahlström[2], Joëlle Rüegg[2], Norbert Giese[1], Madalina Stefan[3], Henning Hopf[3], Ingemar Pongratz[2], Helen Håkansson[4], Gregor Eichele[5], Katarina Pettersson[2] and Heinz Nau[1]

1 Institute for Food Toxicology and Analytical Chemistry, University of Veterinary Medicine, Hannover, Germany
2 Department of Biosciences and Nutrition, Karolinska Institutet, Huddinge, Sweden
3 Institute of Organic Chemistry, Technical University Braunschweig, Germany
4 Institute of Environmental Medicine, Karolinska Institutet, Stockholm, Sweden
5 Max-Planck-Institute for Biophysical Chemistry, Göttingen, Germany

Keywords
dihydro-retinoic acid metabolite; gene expression; novel retinoid metabolites; RAR; vitamin A metabolism

Correspondence
J. P. Schuchardt, Institute of Food Science, Leibniz University of Hannover, Am Kleinen Felde 30, 30167 Hannover, Germany
Fax: +49 511 762 5729
Tel: +49 511 762 2987
E-mail: jan-philipp.schuchardt@lw.uni-hannover.de

(Received 16 December 2008, revised 3 March 2009, accepted 25 March 2009)

doi:10.1111/j.1742-4658.2009.07023.x

Retinoic acid receptor (RAR) and retinoid X receptor are ligand-induced transcription factors that belong to the nuclear receptor family. The receptors are activated by small hydrophobic compounds, such as all-*trans*-retinoic acid and 9-*cis*-retinoic acid, respectively. Interestingly, these receptors are also targets for a number of exogenous compounds. In this study, we characterized the biological activity of the 9-*cis*-substituted retinoic acid metabolite, *S*-4-oxo-9-*cis*-13,14-dihydro-retinoic acid (*S*-4o9cDH-RA). The endogenous levels of this metabolite in wild-type mice and rats were found to be higher than those of all-*trans*-retinoic acid, especially in the liver. Using cell-based luciferase reporter systems, we showed that *S*-4o9cDH-RA activates the transcription of retinoic acid response element-containing genes in several cell types, both from a simple 2xDR5 element and from the promoter of the natural retinoid target gene *RARβ2*. In addition, quantitative RT-PCR analysis demonstrated that *S*-4o9cDH-RA treatment significantly increases the endogenous mRNA levels of the RAR target gene *RARβ2*. Utilizing a limited proteolytic digestion assay, we showed that *S*-4o9cDH-RA induces conformational changes to both RARα and RARβ in the same manner as does all-*trans*-retinoic acid, suggesting that *S*-4o9cDH-RA is indeed an endogenous ligand for these receptors. These *in vitro* results were corroborated in an *in vivo* system, where *S*-4o9cDH-RA induced morphological changes similar to those of all-*trans*-retinoic acid in the developing chicken wing bud. When locally applied to the wing bud, *S*-4o9cDH-RA induced digit pattern duplications in a dose-dependent fashion. The results illustrate that *S*-4o9cDH-RA closely mimics all-*trans*-retinoic acid with regard to pattern respecification. Finally, using quantitative RT-PCR analysis, we showed that *S*-4o9cDH-RA induces the transcription of several retinoic acid-regulated genes in chick wing buds, including *Hoxb8*, *RARβ2*, *shh*, *Cyp26* and *bmp2*. Although

Abbreviations
4o-at-DH-RA, 4-oxo-all-*trans*-13,14-dihydro-retinoic acid; 9c-RA, 9-*cis*-retinoic acid; at-DH-RA, all-*trans*-13,14-dihydro-retinoic acid; at-DH-ROL, all-*trans*-13,14-dihydro-retinol; at-RA, all-*trans*-retinoic acid; at-ROL, all-*trans*-retinol; *bmp2*, bone morphogen protein-2; *Cyp26*, cytochrome P450 26; DR, direct repeat; RA, retinoic acid; RAR, retinoic acid receptor; RARE, retinoic acid response element; *RARβ2*, retinoic acid receptor β 2; RER, relative expression ratio; RXR, retinoid X receptor; RXRE, retinoid X responsive element; *S*-4o9cDH-RA, *S*-4-oxo-9-*cis*-13,14-dihydro-retinoic acid; *shh*, sonic hedgehog; *TBP*, TATA box binding protein.

S-4o9cDH-RA was less potent when compared with all-*trans*-retinoic acid, the findings clearly demonstrate that *S*-4o9cDH-RA has the capacity to bind and activate nuclear retinoid receptors and regulate gene transcription both *in vitro* and *in vivo*.

Retinoids (vitamin A and its analogues) play essential roles in several physiological processes, such as embryonic development, reproduction, immunity, proliferation, differentiation, apoptosis and vision (reviewed in [1–5]). All-*trans*-retinoic acid (at-RA) is the most active naturally occurring retinoid in mammals, except for the visual process, where retinal is the active retinoid form. In the body, at-RA is formed from its precursor all-*trans*-retinol (at-ROL) following a series of reversible and irreversible enzymatic steps (reviewed in [3,6,7]). The biological effects of at-RA are mediated by retinoic acid receptors (RARs) and retinoid X receptors (RXRs) (reviewed in [8,9]). RARs and RXRs are ligand-dependent transcription factors, which belong to different subfamilies of the nuclear receptors (I and II, respectively, according to the official nomenclature [10]). There are different RAR and RXR subtypes (α, β and γ), and each subtype exists in multiple isoforms [11]. at-RA binds to the ligand-binding domain of RARs, which induces heterodimer formation with RXRs to form the transcriptionally active complex. The ligand–receptor–heterodimer complexes act as transcriptional regulators of a multitude of retinoid-regulated genes by binding to specific RA response elements (RAREs) [9,12]. In addition to being heterodimerization partners for RARs, RXRs can also form RXR–RXR homodimers, and regulate the transcription of certain genes via a retinoid X response element (RXRE), characterized by a direct repeat-1 (DR-1) [9,12]. at-RA is responsible for the transcriptional regulation of a multitude of genes, including one of its own receptors: retinoic acid receptor β 2 (*RARβ2*) [13]. This regulation is critical for a number of biological processes, including development and differentiation.

In particular, using developing chick bud as a model, at-RA has been shown to be involved in several facets of normal and abnormal embryogenesis (reviewed in [14]). When at-RA is introduced into the anterior margin of a chick limb bud, it evokes digit pattern duplications in a dose-dependent fashion [15–17]. To bring about these digit duplications, at-RA induces effector genes that regulate limb development. Examples of such genes are bone morphogen protein-2 (*bmp2*) [18], various Hox genes [19–24] and sonic hedgehog (*shh*) [21,25,26]. Cytochrome P450 26 (*Cyp26*; [27,28]) and *RARβ2* [22,23] are also locally induced in the limb bud by exogenously applied at-RA, although their role in normal limb development is not fully understood.

The diverse effects of RA action in controlling miscellaneous cellular processes are thought to be orchestrated by the multiplicity of retinoid metabolizing enzymes and retinoid receptors [3]. The tissue- and cell type-specific varieties of different possible receptor combinations probably control very specific gene pathways influenced by these receptors. Furthermore, the control of retinoid levels is critical, as too high and too low cellular levels of at-RA can have deleterious effects on the organism. Therefore, at-RA is normally rapidly metabolized, which leads to the formation of additional compounds. For example, at-RA is further oxidized for degradation and excretion carried out by three cytochrome P450 enzymes (CYP26 A1, B1 and C1) [29–31]. One interesting question is whether the different retinoid receptors are only activated by at-RA, or whether other endogenous ligands exist, which may regulate gene expression, possibly in a receptor-selective fashion. Studies of retinoid metabolism coupled to gene expression are therefore important to identify novel pathways regulated by noncharacterized active compounds.

Recently, we have isolated and characterized a hitherto unknown endogenous retinoid metabolite, which is present in the liver of mice, rats and humans (Fig. 1B,1) [32]. This metabolite was identified as 4-oxo-9-*cis*-13,14-dihydro-retinoic acid (*S*-4o9cDH-RA), and is characterized by a chiral carbon at C13 (Fig. 1A,3). The identification of *S*-4o9cDH-RA in several tissues of mice, rats and humans is remarkable, as it is the first time a 9-*cis*-configured isomer of RA has been detected endogenously in considerable concentrations. Indeed, some research groups have reported the presence of 9-*cis*-RA (9c-RA [33]) or other 9-*cis*-configured RA metabolites *in vivo* [34–36]. However, the concentrations of these metabolites were much lower than that of at-RA. Moreover, the physiological importance of 9c-RA and other 9-*cis*-configured RA isomers is unclear. Although 9c-RA is known to bind to different RXR isomers [37–41], it is currently questionable whether it could actually be a physiological ligand for RXRs. Two studies have concluded that 9c-RA is most unlikely to be an RXR-activating ligand *in vivo* [42,43]. In contrast with 9c-RA, the endogenous levels of *S*-4o9cDH-RA in serum, kidney and liver of mice and rats were found to be high, reaching micromolar concentrations. In particular, the liver displayed significantly larger amounts of this compound than of

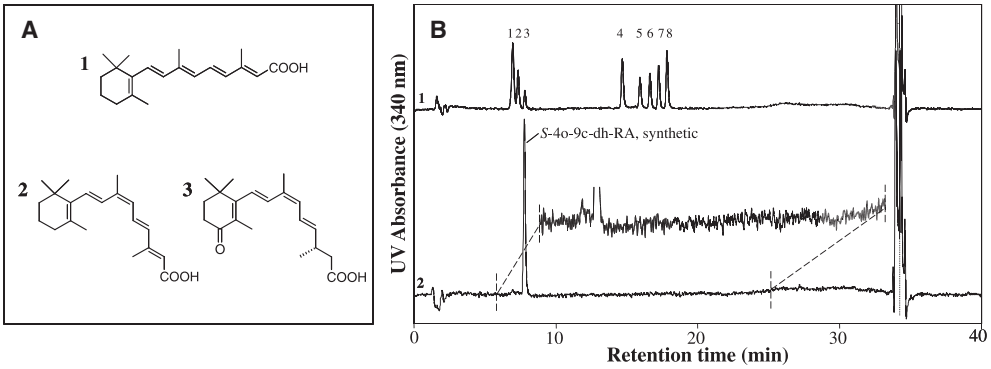

Fig. 1. Chemical structures and chromatograms of polar retinoids separated by reversed-phase HPLC. (A) Chemical structures of at-RA (1), 9c-RA (2) and *S*-4o9cDH-RA (3). (B) Chromatograms of polar retinoids separated by reversed-phase HPLC: 1, polar fraction of liver retinoids from NRMI mice fed with normal diet containing 15 000 IU retinyl palmitate·(kg chow)$^{-1}$; 2, standard mixture consisting of several RA derivatives [1, 4-oxo-13-*cis*-RA; 2, 4-oxo-all-*trans*-RA; 3, *S*-4o9cDH-RA; 4, RO101670 (IS, internal standard; all-*trans*-acitretin); 5, 3,4-didehydro-RA; 6, 13-*cis*-RA; 7, 9-*cis*-RA; 8, at-RA]; 3, aliquot of the synthetic *S*-4o9cDH-RA stock solution used for biological investigations. The 50 times magnification of the signal demonstrates the 100% purity of the stock solution (RP18 column, Spherisorb ODS 2 mm, 2.1 × 150 mm, 3 μm particle size; Waters, Eschborn, Germany).

at-RA. In contrast with at-RA levels, which remain strictly regulated, the endogenous levels of *S*-4o9cDH-RA increased dramatically in the liver following vitamin A supplementation in mice [32]. The physiological relevance of these findings has not been elucidated.

The aim of this study was to investigate whether *S*-4o9cDH-RA is a biologically active retinoid metabolite, using different cell-based model systems and an *in vivo* model. We found that *S*-4o9cDH-RA can activate retinoid-dependent transcription in a dose-dependent manner in both luciferase reporter assays and endogenous genes. In addition, we demonstrated evidence that *S*-4o9cDH-RA is a potential ligand for at least two RAR subtypes, and induces conformational changes of the receptors in the same way as does at-RA. Furthermore, we showed that exogenously applied *S*-4o9cDH-RA mimics the patterning activities of at-RA in the chick limb bud. Finally, using quantitative RT-PCR analysis, we confirmed that *S*-4o9cDH-RA can regulate the expression of several at-RA target genes in the chick wing bud.

Results

S-4o9cDH-RA activates transcription of an RA-responsive reporter gene construct

Previous experiments have shown that the *S*-4o9cDH-RA metabolite is present at high levels in certain tissues, such as the liver, kidney and serum (Fig. 1B,1) [32]. In order to investigate whether *S*-4o9cDH-RA is able to regulate gene transcription via the retinoid receptors, three different cell lines were transfected with a luciferase reporter plasmid under the regulation of a minimal RARE, 2xDR5-luc. All three cell lines express endogenous retinoid receptors, and are therefore suitable model systems for investigating retinoid-dependent signalling. After transfection, cells were treated with increasing doses of synthetic *S*-4o9cDH-RA (Fig. 1B,3) or at-RA, included as a positive control. Stably transfected HC11-RARE (mouse mammary epithelium) cells, treated for 24 h with four concentrations (10 nM to 10 μM) of *S*-4o9cDH-RA, showed a dose-dependent increase in transcriptional activity from the luciferase reporter (Fig. 2A); 1 μM of *S*-4o9cDH-RA induced a significant 1.7-fold increase in transcription compared with the untreated control, and 10 μM resulted in a 2.4-fold increase (Fig. 2A, lanes 5 and 6, respectively). A corresponding 3.2-fold induction was observed in at-RA-treated cells (Fig. 2A, lane 2). Similarly treated, but transiently transfected, HeLa (human cervix carcinoma) cells showed a two-fold increase in transcriptional activity following *S*-4o9cDH-RA treatment at 1 μM (Fig. 2B, lane 6), and treatment with at-RA led to a 3.7-fold increase (Fig. 2B, lane 2). The luciferase activity at low concentrations of *S*-4o9cDH-RA was not significantly induced in these cells. Finally, in P19 (mouse embryonic carcinoma) cells, even low doses of *S*-4o9cDH-RA induced transcription weakly but significantly, and 10 μM led to a 2.8-fold increase (Fig. 2C, lane 7), compared with a 6.8-fold increase following at-RA treatment (Fig. 2C, lane 2). Taken together, *S*-4o9cDH-RA is able to induce transcriptional activity dose dependently. Although the effect of the metabolite was not as potent as that of at-RA, the results were

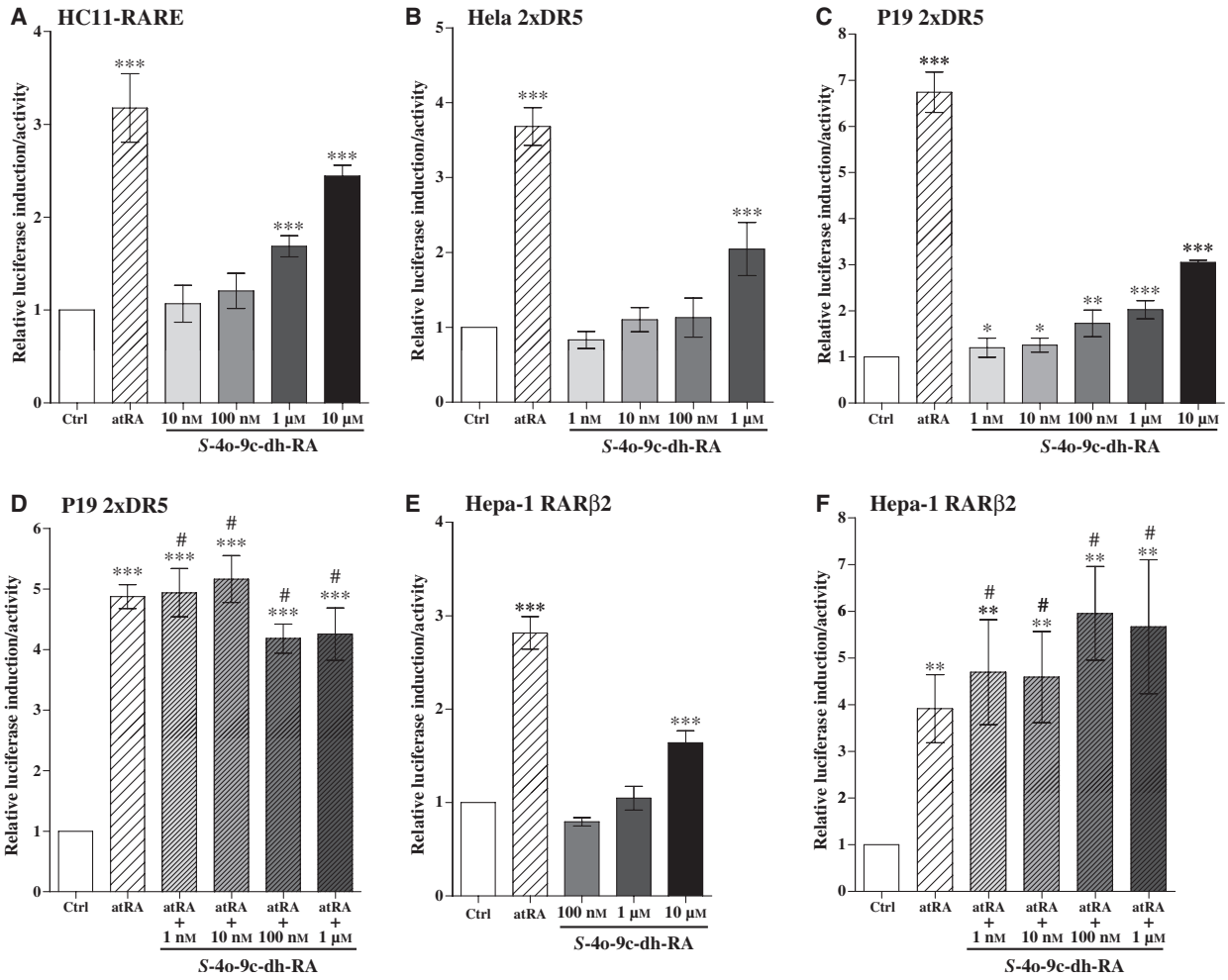

Fig. 2. Transcriptional activation of synthetic and natural RARE by *S*-4o9cDH-RA. HC11, HeLa and P19 cells (A–D) were transfected with a luciferase reporter plasmid regulated by a minimal RARE in direct repeat 2xDR5, whereas Hepa1 cells (E, F) were transfected with a partial region of the gene promoter from the natural retinoid target gene *RARβ2*. Both sequences were cloned into a pGL3basic-luc vector (see Materials and methods for details). As internal control, a vector expressing β-galactosidase was co-transfected. In all the transfection experiments, the cells were transfected for 3 h with the indicated plasmid DNA, except for the stably transfected HC11-RARE cells (A). (A–C, E) Transfected cells treated for 24 h with increasing concentrations of *S*-4o9cDH-RA (as indicated), together with at-RA (100 nM) as a positive control. (D, F) P19 and Hepa1 cells double treated with at-RA and increasing concentrations of *S*-4o9cDH-RA for 24 h. The relative luciferase induction is defined as a quotient of the luciferase levels of treated versus untreated samples. The presented results are the mean values of three experiments carried out in duplicate. Statistical analyses are described in Materials and methods. Asterisks indicate significant difference from untreated controls (Ctrl): $*P < 0.05$; $**P < 0.01$; $***P < 0.001$. #No statistically significant difference between double versus at-RA single treatment.

statistically significant. Next, we analysed the possibility that *S*-4o9cDH-RA could have antagonistic or synergistic effects on at-RA. To investigate this, P19 cells were transfected with the 2xDR5-luc reporter and subsequently treated with at-RA alone (Fig. 2D, lane 2), or in combination with different doses of *S*-4o9cDH-RA, ranging from 1 nM to 1 μM (Fig. 2D, lanes 3–6). All treatments induced significant luciferase reporter activity ($P < 0.001$) between 4.2- and 5-fold. There were no significant differences in transcriptional activity between the cells treated with at-RA alone and the co-treated cells, suggesting that *S*-4o9cDH-RA has neither antagonistic nor synergistic effects, at least in P19 cells.

S-4o9cDH-RA induces transcription from the natural *RARβ2* gene promoter

The results presented above suggest that *S*-4o9cDH-RA can activate RAR/RXR-dependent transcription from a simple synthetic promoter. Next, we investigated the ability of *S*-4o9cDH-RA to activate

transcription from a natural promoter. For this purpose, we chose to use the *RARβ2* gene promoter in a cell line of hepatic origin. Hepa-1 cells, which express endogenous RAR and RXR isoforms, were transiently transfected with the luciferase reporter plasmid pGL3b-RARβluc, containing the natural RA-responsive part of the *RARβ2* promoter. Following transfection, cells were treated with *S*-4o9cDH-RA or at-RA as a positive control. Luciferase reporter activity was induced 1.6-fold compared with the controls following treatment with 10 μM *S*-4o9cDH-RA (Fig. 2E, lanes 1 and 5), whereas the lower concentrations of *S*-4o9cDH-RA had no effect; at-RA-treated cells showed a 2.8-fold increase (Fig. 2E, lane 2). Again, we investigated the possibility of antagonistic or synergistic effects between at-RA and *S*-4o9cDH-RA for activating the retinoid receptors (Fig. 2F). Hepa-1 cells were transfected with pGL3b-RARβluc and treated as the P19 cells in Fig. 2D. In contrast with the results in P19 cells, co-treatment with *S*-4o9cDH-RA resulted in a slight increase in transcriptional activity (Fig. 2F, lanes 3–6). However, as in Fig. 2D, the differences were not significant. Hence, it is not possible to conclude whether *S*-4o9cDH-RA has an antagonistic or synergistic effect on at-RA-induced transcription.

S-4o9cDH-RA activates transcription via both RARα and RARβ

Next, we wanted to investigate whether *S*-4o9cDH-RA displayed RAR isoform specificity. In tissues in which the metabolite is found in high levels (liver, kidney), RARα and RARβ are predominantly expressed, whereas RARγ expression is mainly restricted to skin [44]. Thus, we examined the transcriptional activation of *S*-4o9cDH-RA via RARα and RARβ. CV-1 cells are devoid of retinoid receptors, except for small amounts of RARα. This makes them a useful tool to investigate whether *S*-4o9cDH-RA distinguishes between certain combinations of retinoid receptor isoforms. CV-1 cells were transfected with plasmids expressing a combination of either RARα and RXRβ or RARβ and RXRβ, together with the reporter plasmid 2xDR5-luc. The transfected cells were thereafter treated with at-RA or *S*-4o9cDH-RA, as indicated in Fig. 3A,B. *S*-4o9cDH-RA induced a dose-dependent

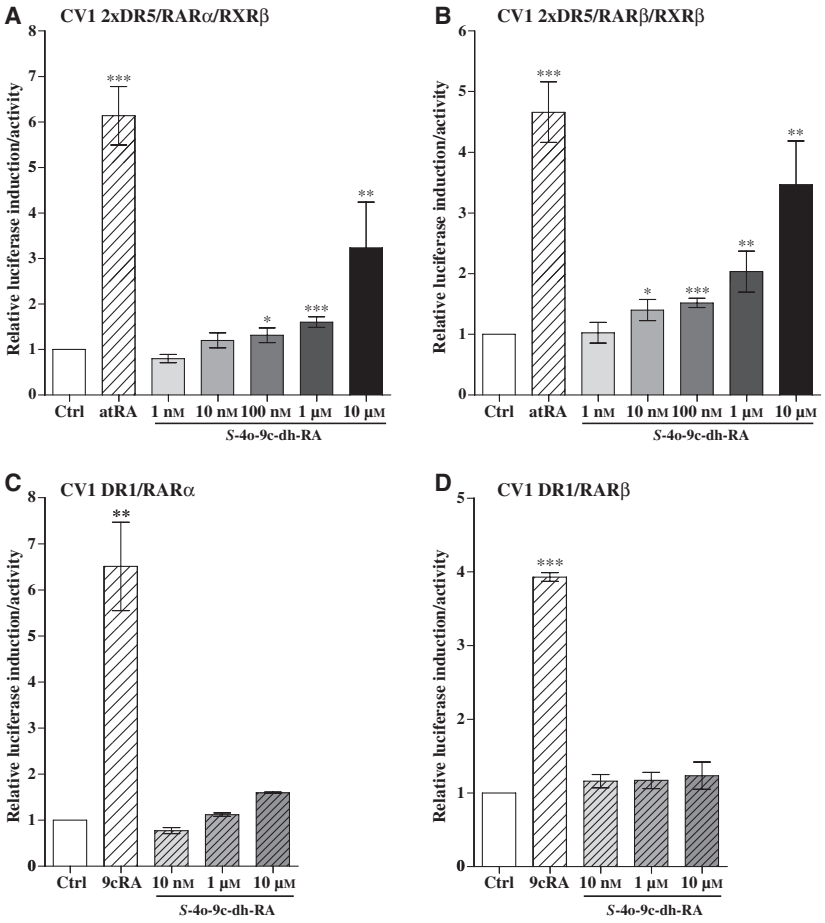

Fig. 3. *S*-4o9cDH-RA transactivates 2xDR5 reporter via RARα/RXRβ or RARβ/RXRβ heterodimers, but fails to transactivate the DR1 element via RXR homodimers in transfected CV1 cells. CV1 cells were transiently co-transfected with the reporter vector pGL3basic2xDR5luc (A, B) or the DR1 element (C, D), together with the expression vectors for RARα and RXRβ (A), RARα and RXRβ (B), RXRα (C) or RXRβ (D). Cells were treated with *S*-4o9cDH-RA at the indicated concentrations. at-RA (100 nM) was used as a positive control in (A) and (B), and 9c-RA (100 nM) was used as a positive control in (C) and (D). Cells were harvested after 24 h of incubation to assay luciferase activity, as described in Materials and methods. The relative luciferase induction is defined as a quotient of the luciferase levels of treated versus untreated samples. The presented results are the mean values of seven experiments carried out in duplicate. Statistical analyses are described in Materials and methods: $*P < 0.05$; $**P < 0.01$; $***P < 0.001$.

transactivation from the 2xDR5 reporter in the presence of both of these combinations of retinoid receptors (Fig. 3A,B). The lowest dose at which a significant increase in transcriptional activation was observed for the RARβ/RXRβ combination was 10 nM (Fig. 3B, lanes 4–7), and at 100 nM for the RARα/RXRβ combination (Fig. 3A, lanes 5–7). At the highest dose of *S*-4o9cDH-RA (10 μM), the fold changes were 3.4- and 3-fold for the RARβ/RXRβ and RARα/RXRβ combinations, respectively, compared with 4.6- and 6.1-fold after at-RA treatment. These results show that *S*-4o9cDH-RA induced transcriptional activation mediated by both of these combinations of retinoid receptors.

To investigate whether *S*-4o9cDH-RA was able to induce transcription via RXRα or RXRβ homodimers, CV-1 cells were transiently transfected with a luciferase reporter containing an RXRE sequence (pGL3b-DR1luc), together with expression vectors for RXRα or RXRβ (Fig. 3B,C). The cells were thereafter treated with 9c-RA (as positive control) or *S*-4o9cDH-RA. The results showed significant reporter activity in response to treatment with 9c-RA, but not with *S*-4o9cDH-RA, suggesting that *S*-4o9cDH-RA is unable to activate transcription of either RXRα or RXRβ homodimers.

S-4o9cDH-RA induces endogenous RAR target gene expression

So far, we have shown that S-4o9cDH-RA is able to activate gene transcription via RAR on transfected promoters. Next, we analysed the ability of this metabolite to activate endogenous gene expression. For this purpose, P19 cells were treated with S-4o9cDH-RA or at-RA for 2 and 24 h. Thereafter, the endogenous mRNA levels of the RAR target gene RARβ2 were analysed using quantitative RT-PCR. After 2 h of treatment, 1 and 10 μM S-4o9cDH-RA induced transcription of endogenous RARβ2 by approximately two- and four-fold, respectively (Fig. 4A, lanes 3 and 4), compared with controls. For both the metabolite and at-RA, the fold change increased significantly with time. After 24 h of treatment with 10 μM S-4o9cDH-RA, the RARβ2 mRNA levels reached a 32-fold increase (Fig. 4B, lane 4) and 1 μM S-4o9cDH-RA resulted in a 3.2-fold increase (Fig. 4B, lane 3), whereas at-RA-treated cells showed 61-fold induction (Fig. 4B, lane 2). The results illustrate that S-4o9cDH-RA is able to induce transcription of retinoid receptor target genes.

S-4o9cDH-RA induces conformational changes of both RARα and RARβ

As *S*-4o9cDH-RA induced retinoid receptor-dependent gene transcription, we wanted to investigate whether the metabolite could bind to these receptors. Ligand binding to nuclear receptors induces a conformational change of the receptor structure, which can be followed using a limited proteolysis assay. The rationale of this experiment is that unliganded and liganded receptors will be degraded differently by proteolytic enzymes, because alternative proteolytic epitopes are exposed as a result of the conformational changes induced by the ligand. As a result, different fragment sizes will be

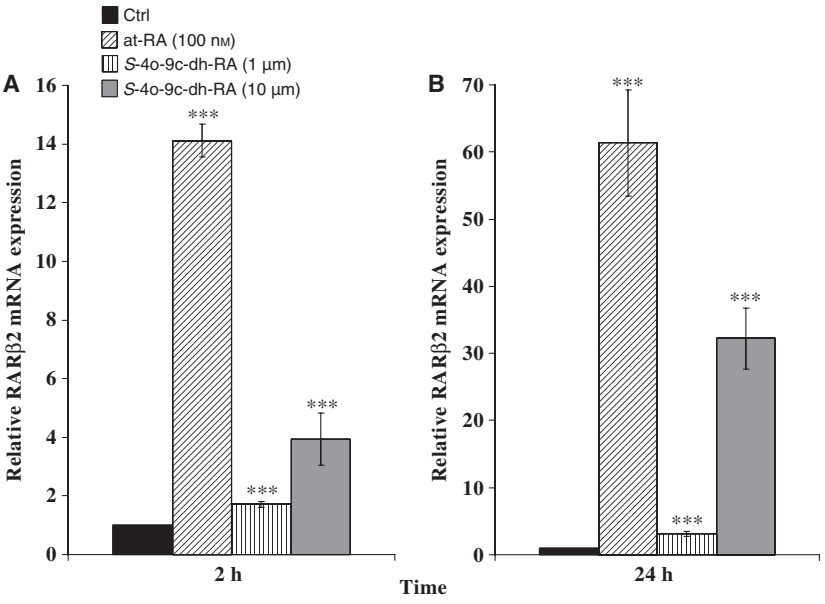

Fig. 4. Induction of endogenous gene transcription in P19 cells by *S*-4o9cDH-RA. P19 cells were simultaneously treated with 1 and 10 μM of *S*-4o9cDH-RA and incubated for 2 h (A) and 24 h (B). As a positive control for RARβ2 induction, cells were treated in parallel with 100 nM at-RA as indicated. PCR primers for RARβ2 and γ-actin were used to analyse the endogenous levels of RARβ2 mRNA (see Materials and methods). The RARβ2 levels in the diagram were calculated using the Δ*C*t method with γ-actin as endogenous control. The presented results are the mean values ± standard error of the mean (SEM) from three experiments. Statistical analyses are described in Materials and methods. Asterisks indicate significant difference from controls: ***$P < 0.001$.

generated from a protease-digested liganded receptor than from an unliganded one. We investigated whether the *S*-4o9cDH-RA metabolite had the ability to induce a distinct conformational change in RARα and RARβ using limited proteolysis analysis. In these experiments, [^{35}S]methionine-labelled RARα and RARβ were translated *in vitro*, incubated with retinoids and digested in limited proteolysis reactions with trypsin. The labelled receptors were incubated with 10 μM *S*-4o9cDH-RA or 100 nM at-RA, or the ethanol vehicle as control, and then digested with trypsin. The results showed that control-treated RARα and RARβ produced a 25-kDa fragment (Fig. 5A,B, lane 4). This fragment was not detectable in samples in which RARα or RARβ had been preincubated with either at-RA or *S*-4o9cDH-RA (Fig. 5A,B, lanes 5 and 6). In the presence of either compound, the receptors demonstrated a different digestion pattern compared with the controls, resulting in the accumulation of a 30-kDa proteolytic fragment. The results suggest that *S*-4o9cDH-RA binds directly to both RARα and RARβ, which, in turn, induces a conformational change of the receptors that resembles that induced by at-RA.

S-4o9cDH-RA alters digit development in a chick embryo model

The observation that *S*-4o9cDH-RA acts similarly to its parent compound at-RA *in vitro* prompted us to test this metabolite in an *in vivo* model. To this end, we used the developing chick wing bud model, a classical model to measure RA action. In this model, at-RA induces digit duplications in a dose-dependent fashion. We analysed whether *S*-4o9cDH-RA had similar effects on the digit pattern. Ion-exchange beads were soaked in ethanolic solutions of *S*-4o9cDH-RA at concentrations ranging from 0.2 to 10 mg·mL^{-1}, and thereafter implanted in the anterior margin of wing buds of Hamburger–Hamilton stage 20 chick embryos. At concentrations of 0.2 and 0.5 mg·mL^{-1}, the wing patterns were mostly normal (Fig. 6A,1) or had an additional digit 2 (Fig. 6A,2). Patterns with additional digits 3 and 4 (43234), in some cases with truncations of digit 2 (4334), became most prevalent when the soaking concentrations were equal to or greater than 1 mg·mL^{-1} (Fig. 6A,3, Table 1). Thus, within a five-fold change in the soaking concentration, there was a dramatic change in effect. The pattern of additional digits was quantified as percentage respecification values (see Materials and methods for a definition), allowing the data to be plotted in a dose–response curve (Fig. 6B). The efficacy of at-RA in the limb pattern duplication assay has been extensively

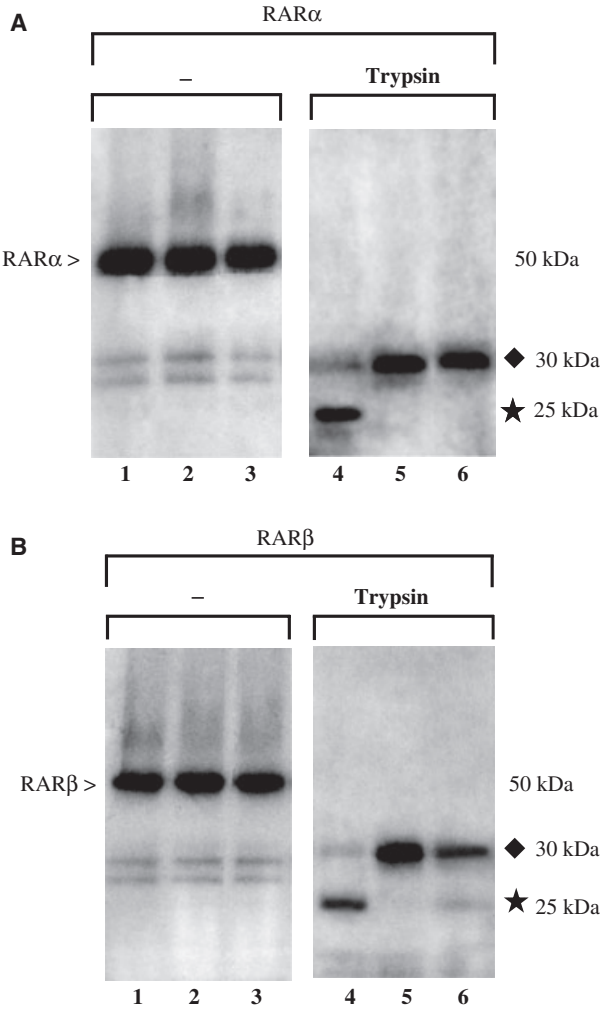

Fig. 5. *S*-4o9cDH-RA inhibits limited trypsin digestion of RARα and RARβ. *In vitro*-translated [^{35}S]methionine-labelled RARα (A) and RARβ (B) samples were pre-incubated with ethanol alone (A, lanes 1 and 4; B, lanes 1 and 4) or together with 100 nM at-RA (A, lanes 2 and 5; B, lanes 2 and 5) or 10 μM *S*-4o9cDH-RA (A, lanes 3 and 6; B, lanes 3 and 6), followed by incubation with trypsin or buffer only as indicated (for details, see Materials and methods). Samples were separated by 10% SDS–PAGE/fluorography. For both RARα and RARβ, the 30 kDa proteolytic fragments (marked by a diamond) of the receptors were protected from digestion by the presence of either retinoid (A, lanes 5 and 6; B, lanes 5 and 6), in comparison with the samples treated with ethanol only (A, lane 4; B, lane 4). The 25 kDa fragments of the trypsin-digested receptors (marked by a star) were only present in the samples treated as controls (ethanol; A, lane 4; B, lane 4).

documented (e.g. [16,17]). As can be seen in the dose–response curves, the profile for *S*-4o9cDH-RA (marked by filled circles) was shifted towards higher soaking concentrations and did not reach the same maximal response, indicating that this RA metabolite has a lower potency than at-RA by a factor of

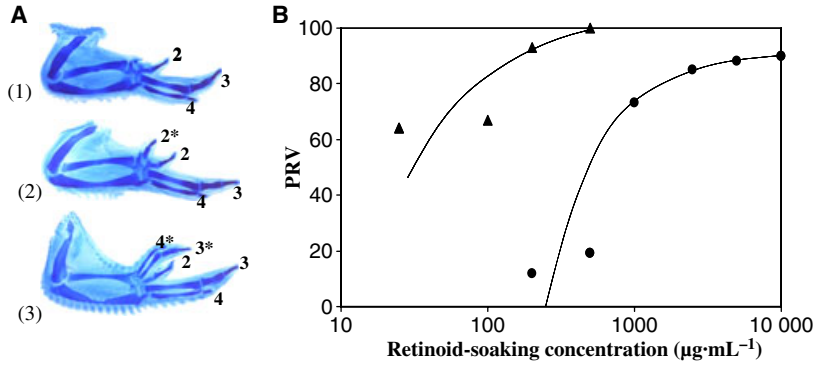

Fig. 6. Effect of different doses of locally applied *S*-4o9cDH-RA (circles) and at-RA (triangles) on the chick wing pattern and dose–response curves. (A) Beads were soaked in ethanolic *S*-4o9cDH-RA solution and implanted at the anterior margin of the right wing buds of stage 20 chick embryos. The images display the most frequent wing digit patterns of the chick embryos in the different treatment groups. 1, Normal 234 pattern (untreated control and soaking concentration of 0.2 mg·mL^{-1}; 2, 2234 pattern (concentration, 0.5 mg·mL^{-1}); 3, 43234 pattern (concentration, 1 mg·mL^{-1}). Digit identities 2, 3, 4 are read from anterior to posterior; additional digits are marked by asterisks. (B) The percentage respecification value (PRV) was plotted against the soaking concentration and is a measure of the extent of pattern duplication (for definition, see Materials and methods). PRV is an average value of each set. The sum of the scores of each wing is divided by the number of limbs in each set.

approximately 15. It should also be noted that *S*-4o9cDH-RA did not evoke the loss of hand plate or forearm elements, a result frequently seen with high doses of at-RA (Table 1 and [17]). Thus, the novel RA metabolite is less embryotoxic than at-RA. Control bead implants immersed in ethanol had no effect on the wing digit pattern (Table 1).

S-4o9cDH-RA induces the expression of RA-regulated genes in the limb bud

To examine the regulation of genes involved in normal limb development, beads soaked in 0.2 mg·mL^{-1} at-RA or 2 mg·mL^{-1} *S*-4o9cDH-RA were implanted in the limb buds. These concentrations were selected because they evoked pattern duplications to a similar extent (about 90% respecification value) by the two retinoids (Table 1; Fig. 7B). Transcript levels of the direct at-RA target genes *RARβ2*, *Cyp26* and *Hoxb8* were determined by quantitative RT-PCR in whole buds removed after 6 h of retinoid treatment. Transcripts of the indirect at-RA target genes *shh* and *bmp2* were quantified in buds treated for 24 h, as their induction by at-RA is known to occur only after prolonged treatment [18,21]. As endogenous *shh* is expressed only in the posterior part of the limb bud [25], buds were dissected into posterior and anterior halves prior to RNA isolation, and induction was assessed in both halves independently. *bmp2* transcript levels were also measured in both halves because, in the Hamburger–Hamilton stages between 17 and 26, the occurrence of *bmp2* transcripts is also mostly restricted to the posterior mesenchyme [18]. Transcript levels of all investigated retinoid-regulated target genes were increased significantly in limb bud tissue treated with either retinoid (Fig. 7A–E); 2 mg·mL^{-1} of *S*-4o9cDH-RA induced *RARβ2*, *Cyp26* and *Hoxb8* by 2.1-, 5.7- and 2.3-fold, respectively (Fig. 7A–C, lane 2), and at-RA induced 2.3-, 8.9- and 2.2-fold changes, respectively (Fig. 7A–C, lane 3). Thus, *Hoxb8* expression was somewhat more induced by *S*-4o9cDH-RA than by at-RA (Fig. 7C), whereas *RARβ2* and *Cyp26* were slightly less induced by *S*-4o9cDH-RA than by at-RA (Fig. 7A,B).

The indirect target genes *bmp2* and *shh* were also induced by both retinoids (Fig. 7D,E). In the anterior limb bud half, *bmp2* was significantly induced by 1.9-fold with *S*-4o9cDH-RA (Fig. 7D, lane 2) being more efficient than at-RA (Fig. 7D, lane 3: 1.3-fold). Endogenously, the expression of *shh* is restricted to the posterior half of the limb buds. However, both retinoids induced the expression of *shh* in the anterior section. As there is no endogenous expression of *shh* in the anterior tissue, the relative expression ratio (RER) for *shh* (RER$_{shh}$) in Fig. 7E is determined as a quotient between at-RA- and *S*-4o9cDH-RA-treated samples. By this criterion, at-RA induced *shh* six-fold more strongly than did *S*-4o9cDH-RA. There was no difference found in the expression of target genes in untreated limb bud samples and samples treated with ethanol-soaked beads (data not shown). In conclusion, *S*-4o9cDH-RA is able to control the expression of genes involved in limb morphogenesis, such as *shh* [25], *Hoxb8* [19,20] and *bmp2* [18], and likewise induces the expression of direct at-RA-regulated target genes, such as *RARβ2*, *Cyp26* and *Hoxb8*.

Table 1. Digit patterns following local application of at-RA or *S*-4o9cDH-RA to stage 20 chick wing buds. PRV, percentage respecification value.

Treatment	Soaking concentration (mg·mL^{-1})	Embryos per group (*n*)	Digit pattern[a]	Number of cases	PRV
at-RA	0.025	12	234 (normal)	1	64
			d234	1	
			*dd*234, dd234, *d32*34	3	
			*43*234, 43234	7	
	0.1	8	*22*34, 2234	4	67
			43234, *43*234	4	
	0.2	9	*22*34	1	93
			*43*234	2	
			4334	6	
	0.5	8	234	1	100
			4334, *433*4	3	
			434	1	
			Humerus only	3	
S-4o9cDH-RA	0.2	8	234 (normal), d32	6	12
			2234	2	
	0.5	7	234 (normal)	3	19
			2234, d234	4	
	1	10	2234	3	73
			dd234	1	
			43234	5	
			4334	1	
	2.5	9	2234	1	85
			dd234	1	
			*4d*234	1	
			43234, *43*234, *43*234	6	
	5	11	2234, *22*34	2	88
			43234, *43*234, *43*234	7	
			4d234	1	
			*43d*234	1	
	10	13	*dd*234	2	90
			43234, *43*234	10	
			4334	1	
Ethanol		8	234 (normal)	8	0

[a] Digit identities are read from anterior to posterior; digits which are not clearly identifiable are marked as 'd'; digits which are proximally fused are shown in italic.

Discussion

The number of identified endogenous retinoid receptor ligands in plasma and/or soft tissues of various species, including humans, is limited. Over recent years, several studies have been published that have aimed to discover novel endogenous RA metabolites with receptor binding affinity by providing retinoids exogenously [34,36,45]. For example, Shirley *et al.* [36] described the reduction of 9c-RA to 9-*cis*-13,14-dihydro-RA in rat plasma after the administration of 9c-RA, and Moise *et al.* [45] reported the occurrence of all-*trans*-13,14-dihydro-RA in the liver of transgenic mice supplemented with retinyl palmitate. Recently, we found endogenous levels of *S*-4o9cDH-RA in both wild-type mice and rats fed with a standard laboratory diet, as well as in humans, with high levels being present primarily in the liver, but also in other tissues [32].

The physiological role of oxidized RA metabolites is not clearly understood. Although oxidation is generally viewed to be the first step in the elimination pathway for at-RA *in vivo*, it has been shown that the metabolite 4-oxo-all-*trans*-RA is a highly active modulator in embryonic development [46]. Furthermore, 4-OH-all-*trans*-RA, 4-oxo-all-*trans*-RA and 5,6-epoxy-all-*trans*-RA are other oxidative metabolites that exhibit significant biological activity in various types of cell line [47–49]. These studies demonstrate a putative role of retinoid metabolites in diverse biological processes. However, a later study has provided genetic evidence that oxidative RA metabolites are not required for physiological retinoid signalling [50]. This study was carried out on mice lacking CYP26A1, the enzyme that

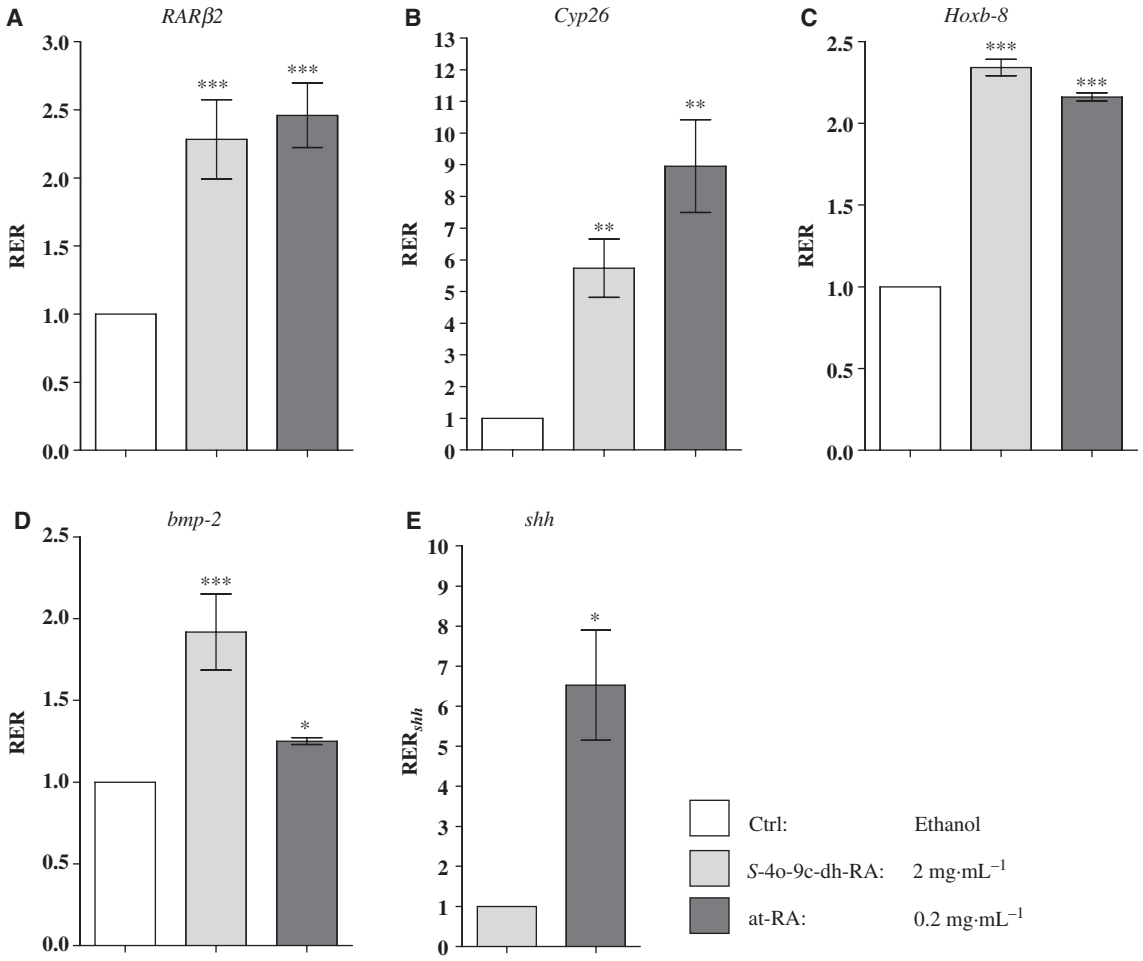

Fig. 7. Transcript levels of RA-induced genes in limb bud tissue. Transcript levels of direct at-RA target genes (A–C, *RARβ2*, *Cyp26*, *Hoxb8*) and indirect at-RA target genes (D, E, *bmp2*, *shh*) induced in limb buds treated with *S*-4o9cDH-RA or at-RA. Beads were soaked in a solution of 2 mg·mL^{-1} *S*-4o9cDH-RA or 0.2 mg·mL^{-1} at-RA, respectively. Absolute expression levels were determined by the standard curve method (see Materials and methods). RER values of target genes were normalized to TBP (target gene/TBP). (A–D) Transcript levels, expressed as RERs, of treated buds were compared with the endogenous expression levels of the appropriate genes in untreated buds (Ctrl). (E) RER_{shh} was determined as a quotient between at-RA- and *S*-4o9cDH-RA-treated samples (see Materials and methods). The presented results are the mean values of three experiments carried out in duplicate. Statistical analyses are described in Materials and methods. Asterisks indicate significant difference from controls (Ctrl): $*P < 0.05$; $**P < 0.01$; $***P < 0.001$.

metabolizes at-RA into more polar hydroxylated and oxidized derivatives. The mice display severe developmental abnormalities, for example spina bifida, which theoretically could result either from an excess of at-RA caused by a lack of tissue-specific catabolism, or from a lack of signalling by bioactive RA metabolites, such as 4-oxo-all-*trans*-RA. The authors demonstrated that the former is the case, as these mice were phenotypically rescued by heterozygous disruption of the RA-synthesizing enzyme, retinal dehydrogenase 2, i.e. by reducing the at-RA levels. This study illustrates the importance of tightly regulating at-RA levels in the body. This can also be achieved by circumventing at-RA synthesis from its precursor at-ROL, which has been demonstrated to occur in mice [45]. Mice deficient in lecithin:retinol acyltransferase, an enzyme involved in the esterification and storage of at-ROL [51], showed increased levels of 13,14-dihydro-retinoids after the administration of high retinyl palmitate contents in the diet [45]. Thus, the formation of 13,14-dihydro-retinoid metabolites, such as *S*-4o9cDH-RA, could be a further degradation pathway to protect the body against pharmacological doses of at-ROL as a result of fluctuations in nutritional vitamin A (predominantly at-ROL) levels, under circumvention of the formation of at-RA. This could be an explanation of the strongly increasing *S*-4o9cDH-RA and relatively stable at-RA levels in mice gavaged with retinyl palmitate at high doses [32].

Nevertheless, the enzymatic pathways responsible for the formation of *S*-4o9cDH-RA and the possible precursor retinoids are not known. The metabolism of vitamin A is a highly regulated process, which includes conjugation, decarboxylation, oxidation, double bond isomerization and reduction, carried out by a well-organized interplay of enzymes, as well as inter- and extracellular retinoid binding proteins [3]. A novel enzyme, described in mice [52], could possibly catalyse the key step in the formation of 13,14-dihydro-RAs. All-*trans*-retinol : 13,14-dihydroretinol saturase converts at-ROL to at-DH-ROL. Likewise, it has been demonstrated that the same enzymes involved in the oxidation of at-ROL to at-RA and then to oxidized RA metabolites can also catalyse the oxidation of the corresponding dihydro-metabolite at-DH-ROL to oxidized dihydro-RAs [45]. These synthesizing and metabolizing enzymes are involved in the combined regulation of desirable at-RA levels, and could likewise be involved in the formation of *S*-4o9cDH-RA under certain physiological circumstances. However, this potential metabolic pathway is not sufficient to explain why *S*-4o9cDH-RA is 9-*cis*-configured.

At present, the physiological role of 9c-RA is still unclear. 9c-RA is normally undetectable in mammals, except when vitamin A is present in excess [42,53], although it can potentially be synthesized by presently known enzymes, or derived from isomerization of at-RA [54]. Heymann *et al*. [33] reported the occurrence of relative high 9c-RA levels in the liver and kidney of untreated wild-type mice. However, these findings could not be reproduced by other laboratories. In an earlier study, we reported, for the first time, detectable amounts of 9c-RA and 9,13-di-*cis*-RA in human plasma, but only after consumption of liver or vitamin A supplementation [53]. However, the plasma levels of 9c-RA after liver consumption decreased within a few hours to levels at or below the analytical detection limit. It is still unclear whether 9c-RA is present endogenously in mammalian blood or tissue, including the embryo. If at all, the concentrations appear to be very low. Considering these facts, the role of 9c-RA in retinoid signalling pathways as a putative RXR ligand is difficult to evaluate. 9c-RA may rather play a pharmacological than a physiological role as an RXR ligand [3].

The finding that a 9-*cis*-configured metabolite – *S*-4o9cDH-RA – occurs endogenously and, moreover, at high levels, which fluctuate depending on the retinol intake, prompted us to examine whether *S*-4o9cDH-RA plays a physiologically relevant role in retinoid signalling. Data from preliminary molecular modelling calculations suggest that *S*-4o9cDH-RA could act as a potential ligand for both RXR and RAR receptors, as its three-dimensional structure and geometry can adopt a conformation which fits the ligand binding pockets of the two receptors (M. Stefan, unpublished results). In this study, we confirmed that *S*-4o9cDH-RA can activate transcription via RAR–RXR heterodimers, whereas the metabolite cannot induce transcriptional activity of either RXRα or RXRβ. We have shown that *S*-4o9cDH-RA can activate gene transcription via the retinoid receptors in a similar fashion as at-RA, although to a lesser extent. As a result of the ascertained purity of the synthetic *S*-4o9cDH-RA used in the experiments, it can be excluded that the effects were falsified by any other active RA.

S-4o9cDH-RA was able to activate transcription in the presence of two different combinations of retinoid receptors, suggesting that it displays no apparent isoform selectivity for RARα or RARβ. As RARγ expression is mainly restricted to skin [44], and the primary occurrence of *S*-4o9cDH-RA is restricted to the liver, we focused our study on the α and β isoforms. In addition to its transcriptional effects, *S*-4o9cDH-RA induced conformational changes in both RARα and RARβ in a limited proteolysis assay in the same manner as at-RA. Taken together, these observations indicate that *S*-4o9cDH-RA functions as a *bona fide* ligand for both RARα and RARβ and hence activates RAR-dependent gene transcription. Our data provide no indication that *S*-4o9cDH-RA possesses either antagonistic or synergistic effects towards those of at-RA.

Using the chicken limb bud model, we demonstrated that *S*-4o9cDH-RA is biologically active and induces morphological changes similar to those reported for at-RA [15–17,55,56]. It has been proposed that the role of at-RA during the complex interactions and morphogenetic processes in limb development is a result of the initiation of a cascade of events involving signalling molecules, which bring about the formation of additional digits, when expressed together [21]. The assumption that *S*-4o9cDH-RA provokes digit duplication in the same way as at-RA is supported by our finding that *S*-4o9cDH-RA can control the expression of several genes involved in limb morphogenesis, including *shh* [25], *Hoxb8* [19,20] and *bmp2* [18]. In addition, *S*-4o9cDH-RA induces the expression of *RARβ2*, *Cyp26* and *Hoxb8*, which are known to be direct retinoid target genes [57–60].

Our *in vitro* and *in vivo* data suggest that *S*-4o9cDH-RA is an activator for retinoid-dependent signal transduction, although less potent than at-RA when using solution concentrations as a reference value. There are several explanations for the comparatively lower efficacy of the metabolite. An apparent explanation is the lower binding affinity and thus transactivational capacity of

S-4o9cDH-RA. However, it is difficult to draw this conclusion because the metabolic stability of *S*-4o9cDH-RA is not known. It is possible that at-RA is more metabolically stable in the systems used in this study, and thus the actual tissue concentrations of *S*-4o9cDH-RA and at-RA are comparable. Therefore, the difference in metabolic clearance may account for the difference in efficacy in the present study. To gain further information about the metabolic stability of *S*-4o9cDH-RA, it will be necessary to measure the clearance of *S*-4o9cDH-RA in comparison with at-RA using radiolabelled compounds. Furthermore, in our previous study, we showed that the concentration of *S*-4o9cDH-RA in mice liver exceeded that of at-RA; thus, it is possible that, in the organism, the metabolite reaches local concentrations that are sufficient to activate RAR signalling.

From the results presented in this study, we suggest that *S*-4o9cDH-RA is a biologically active retinoid metabolite that may have gene regulatory functions under physiological conditions. However, in order to establish the physiological role of *S*-4o9cDH-RA, further studies are necessary. It is important to understand the formation and degradation of *S*-4o9cDH-RA. The use of recombinant enzymes and siRNA against enzymes possibly involved in the formation of *S*-4o9cDH-RA could be a suitable technique to reconstitute the pathway of the new metabolite *in vitro*. Knockout animals, deficient in certain enzymes involved in the metabolism of retinoids, could also be an appropriate way to answer these questions *in vivo*. Likewise, it needs to be determined whether *S*-4o9cDH-RA has specific biological roles other than those similar to at-RA. Interestingly, the hepatic levels of *S*-4o9cDH-RA increase drastically as a consequence of a high retinyl palmitate content in the diet. A similar correlation to dietary intake was not seen for at-RA, for which the levels are very strictly regulated. Tissue levels of *S*-4o9cDH-RA are most likely similarly influenced by dietary vitamin A intake in humans, suggesting a specific role of *S*-4o9cDH-RA in retinoid-dependent gene regulation directly connected to dietary intake, which has not been demonstrated for at-RA.

Materials and methods

Material

at-RA was purchased from Sigma-Aldrich (Steinheim, Germany). *S*-4o9cDH-RA was synthesized according to a developed enantioselective reaction series, which will be published elsewhere. All retinoids used were diluted in ethanol. The stock solutions were regularly checked for purity using reversed-phase HPLC analysis, as described previously [61]. Figure 1B demonstrates the chemical purity of an aliquot of synthetic *S*-4o9cDH-RA (Fig. 1B,3) used in the experiments, in comparison with a standard mixture of several RA derivatives (Fig. 1B,2) separated by reversed-phase HPLC. Prior to each experiment, retinoid stock solutions were diluted in culture medium to the final exposure concentration. All experimental procedures involving treatment with retinoids were light-protected.

Plasmid constructs

The 2xDR5-luc reporter plasmid was constructed using two copies of a consensus RARE ($AGGTCAn_5AGGTCA$) placed in front of a minimal TATA box and inserted into the pGL3basic vector (Promega, Nacka, Sweden). The pGL3b-RARβ2luc reporter contains the natural RA-responsive *RARβ2* gene promoter (– 180 to + 83) inserted into the pGL3basic vector. The plasmids expressing different retinoid receptors (RARα and β, RXRα and β) have a pSG5 backbone.

Cell culture and transient transfections

Green monkey kidney cells (CV1), mouse embryonic carcinoma cells (P19) and human cervix carcinoma cells (HeLa) were routinely maintained in high-glucose Dulbecco's modified Eagle's medium (DMEM; Gibco Invitrogen, Carlsbad, CA, USA) supplemented with 10% (v/v) fetal bovine serum (Gibco Invitrogen), 1% (v/v) PEST (Gibco Invitrogen), 1% (v/v) L-glutamine (Gibco Invitrogen) and 1% nonessential amino acids (Gibco Invitrogen). Murine hepatoma-1 cells (Hepa-1c1c7; Hepa-1) were grown in low-glucose DMEM (Gibco Invitrogen) supplemented with 10% (v/v) fetal bovine serum (Gibco Invitrogen), 1% (v/v) PEST (Gibco Invitrogen), 1% (v/v) L-glutamine (Gibco Invitrogen) and 1% (v/v) pyruvate (Gibco Invitrogen). Mouse mammary epithelial cells (HC11) were grown in RPMI 1640+ medium (Gibco Invitrogen) supplemented with 1% (v/v) gentamicin (Gibco Invitrogen), 1% (v/v) L-glutamine, 5 $\mu g \cdot mL^{-1}$ insulin (Gibco Invitrogen), 10 $ng \cdot mL^{-1}$ epidermal growth factor (Gibco Invitrogen) and 240 $\mu g \cdot mL^{-1}$ Geneticin® (G418; Gibco Invitrogen). P19 cells were grown on culture plates pre-treated with 0.1% gelatin (w/v in water). The day before transfection, cells were seeded on 12- or 24-well culture plates. Transient transfections were performed using lipofectamine™ and Plus Reagent (Invitrogen, Carlsbad, CA, USA), according to the manufacturer's protocol, in serum and antibiotic-free media. Briefly, each well received 100 ng of reporter plasmid (as indicated in the figure legends) and 20 ng of a CMV-β-galactosidase expressing plasmid (serving as an internal control for transfection efficiency) and, in the case of CV1 cells, 5–20 ng of expression plasmids for RARα, RARβ, RXRα or RXRβ as indicated. After 3 h, media containing serum and retinoids (1 nM to 10 μM S-4o9cDH-RA; 100 nM at-RA and 9c-RA) were added and the cells

were incubated for 24 h, when the media were removed and the cells were harvested. Luciferase activity was measured using a Luciferase assay kit (BioThema AB, Haninge, Sweden), according to the manufacturer's instructions, employing an automated luminometer (Lucy 3; Anthos Labtec Instruments, Salzburg, Austria). β-Galactosidase activity was determined using the Tropix Galacto-Light Plus chemiluminescence assay system (Tropix, Bedford, MA, USA), according to the manufacturer's protocol. Data are presented as the mean ± standard deviation (SD) of relative luciferase activity corrected for the internal standard of, in each case, at least three experiments performed in duplicate.

Stable transfections

For stable transfections, HC11 cells were grown in 10-cm plates and transfected with 10 μg of the pGL3b-2xDR5luc reporter plasmid using lipofectamine^{TM} reagent (Invitrogen). Stable clones were selected in 240 $\mu g \cdot mL^{-1}$ geneticin in RPMI 1640 medium.

Induction of *RARβ2* mRNA in P19 cells

P19 cells were allowed to aggregate on six-well plates for 1 day before the start of each experiment. The subsequent incubation with the indicated retinoids was then terminated at the indicated time points by washing with NaCl/P_i and lysis of the cells using 1 mL of Trizol (Invitrogen) per well. Total RNA from the cells was extracted according to the manufacturer's protocol. In order to eliminate genomic DNA, 2 g of total RNA from each extracted sample was treated with DNaseI (Invitrogen) before cDNA synthesis (SuperScriptII; Invitrogen). Quantitative real-time PCR was performed using Power CyberGreen MasterMix (Applied Biosystems, Foster City, CA, USA) in a total volume of 12 L, including 2 L of cDNA template diluted five times in water, and 300 nM of forward and reverse primer. ABI Prism 7500 Fast Sequence Detection System instrument and software (v1.3) (Applied Biosystems) were used to amplify and analyse specific mRNA expression, with a reaction profile of 95 °C for 10 min, followed by 40 cycles of 95 °C for 15 s and 60 °C for 60 s. A dissociation curve analysis was added to each run in order to trace artefacts in individual samples. Each cDNA template was analysed in duplicate and the results represent three separate experiments. The forward and reverse PCR primers for *RARβ2* and γ-actin have been published elsewhere [62].

Limited proteolytic digestion of *in vitro*-translated receptors

[^{35}S]Methionine (Amersham Biosciences AB, Uppsala, Sweden)-labelled mouse RARα and RARβ proteins were synthesized *in vitro* using the coupled rabbit reticulocyte lysate cell-free system (Promega), according to the instructions provided by the manufacturer, using the expression vectors pSG5-RARα and pSG5-RARβ as templates. Aliquots of reticulocyte lysates containing [^{35}S]methionine-labelled RARα or RARβ were incubated with 100 nM at-RA or 10 μM *S*-4o9cDH-RA for 45 min at 30 °C. Controls were incubated with vehicle (0.05% ethanol). To 5 μL aliquots of retinoid-treated receptor proteins, 4 μL of trypsin (Promega) dissolved in 50 mM acetic acid buffer was added and incubated for 10 min at 25 °C. The reaction was stopped by the addition of 6 μL of 5 × SDS loading buffer containing 500 μM EDTA and boiling of the samples for 5 min prior to separation on 10% (w/v) SDS-polyacrylamide gels. For fixation of the proteins, the gels were soaked in 25% isopropyl alcohol and 10% acetic acid aqueous solution for 30 min, followed by Amplify (Amersham) for 30 min. After drying, the gels were autoradiographed overnight at − 80 °C.

Local application of RA to chick embryos

Fertilized White Leghorn chicken eggs (VALO specified pathogen-free eggs; Lohmann Tierzucht, Cuxhaven, Germany) were incubated at 37.5 °C and a humidity of approximately 60%. After 65 h of incubation in a horizontal orientation, eggs were windowed, and embryos were staged according to Hamburger & Hamilton [63]. Approximately 15 AG1-X2 ion-exchange beads (Bio-Rad, Richmond, CA, USA) (diameter, 200–250 μm) were placed by forceps into a 1.5 mL microcentrifuge polypropylene tube and soaked in 30 μL ethanolic solution containing the retinoids. The soaking concentration for at-RA ranged from 25 to 500 $\mu g \cdot mL^{-1}$ for limb duplication experiments and 200 $\mu g \cdot mL^{-1}$ for gene expression analysis. The soaking concentration for *S*-4o9cDH-RA was 0.2–10 $mg \cdot mL^{-1}$ for limb duplication experiments and 2 $mg \cdot mL^{-1}$ for gene expression analysis. Control beads were soaked in ethanol alone. The microcentrifuge tubes containing beads were vigorously shaken in a microtube shaker for 20 min at room temperature. After removing the retinoid solution, the beads were washed twice for 20 min in 200 μL of phenol red-containing phosphate-buffered saline (100 mL NaCl/P_i and 500 μL of a 2 $mg \cdot mL^{-1}$ phenol red solution in ethanol). Beads were then implanted using watchmaker's forceps (type 5) underneath the apical ectodermal ridge at the anterior margin of the right limb bud of a Hamburger–Hamilton stage 20 chick embryo (for details, see [17]). The eggs were sealed with tape and returned to the incubator for either 6 or 24 h for gene expression analysis and 7 days for analysis of wing patterns.

Analysis of wing patterns and dissection of limb bud tissue

After 7 days of incubation, embryos were sacrificed, washed three times in water, fixed in 5% (w/v) trichloroacetic acid

(Roth, Karlsruhe, Germany), stained in Alcian blue dye (Sigma-Aldrich, Steinheim, Germany) solution [0.5 g of dye in 500 mL of 70% (v/v) ethanol containing 1% HCl], differentiated in acidic ethanol (70% ethanol containing 1% HCl) and cleared with methyl salicylate (Sigma-Aldrich). In order to generate dose–response curves that quantitatively reflect the effects, the extent of pattern duplication was stated in percentage respecification values, in which the wing patterns were expressed in numerical terms. Patterns were scored as follows: a pattern with the anterior-most additional digit being a digit 4 scored 100%; a wing with an additional digit 3 anteriorly scored 66%; a wing with an additional digit 2 scored 33%; a digit of equivocal identity obtained a score of 0%. For the analysis of limb buds, embryos were dissected out of the egg after 6 and 24 h of incubation and rinsed in ice-cold NaCl/P_i. The buds were cut off with small scissors. Whole buds were used from the 6 h time point, whereas buds from the 24 h time point were cut into anterior and posterior parts using a fine tungsten needle. For each time point, three buds were pooled, and experiments were carried out in triplicate. Dissected buds were collected in microcentrifuge vials and immediately rinsed in a tissue disruption buffer (RNeasy®, Qiagen, Hilden, Germany).

RA target gene expression analysis in limb tissue

Total RNA was extracted and purified using a universal tissue RNeasy® Kit (Qiagen), according to the manufacturer's instructions. Total RNA was reverse transcribed (ThermoScript™ RT-PCR-System; Invitrogen) using oligo-$(dt)_{20}$ primers, as described in the protocol provided. To limit variations, all RNA samples were reverse transcribed isochronal. Quantitative RT-PCR was performed on an iCycler™ (Bio-Rad, Hercules, CA, USA) in 20 μL reaction mixtures with 350 nM of each primer and iQ SYBRGreen Supermix (Bio-Rad, Munich, Germany), following the manufacturer's instructions. Real-time PCR conditions consisted of an initial denaturation step at 95 °C for 10 min, followed by 50 cycles of denaturation for 15 s at 94 °C, annealing for 25 s at 60 °C and extension for 20 s at 72 °C, with a single fluorescence measurement. The specificity of the quantitative RT-PCR products was determined by performing melting curve analysis after each PCR from 50 to 94 °C with an increasing set point temperature after cycle 2 by 0.5 °C·s^{-1} and continuous fluorescence measurement. Oligonucleotide primers specific for *Hoxb8* (sense, 5′-CTACCAGACGCTGGAACTGG; antisense, ACCTGCCTTTCTGTCAATCC), *Cyp26* (sense 5′-CTTTCAGTGGGCTCTACCG; antisense, GCAGTGC ATCCTTGTAGCC), *RARβ2* (sense, 5′-GCATGCTTCAGT GGATTGG; antisense, AGTGGTGAAGGAGGGCTTG), *shh* (sense, 5′-GGCCAGTGGAAGATATGAAGG; antisense, GCATTCAGCTTGTCCTTGC), *bmp2* (sense, 5′-CC TACATGTTGGACCTCTATCG; antisense, AAACTTCTT CGTGGTGGAAGC) and TATA box binding protein (*TBP*) (sense, 5′-CTGGCAGCAAGGAAGTACG; antisense, GCTCATAGCTGCTGAACTGC) were designed using the software Primer3 and optimized to an annealing temperature of 60 °C. *TBP* is a housekeeping gene that should be equally expressed in all cells and was used as an internal standard. Expression levels of target genes were determined by the standard curve method. The standard curve of each target gene was obtained with coincidental samples over 3.5 log levels on each plate. The absolute quantity of target RNA was determined by iCycler™ iQ optical software (Bio-Rad, Hercules, CA, USA). The expression level of each target gene was normalized by dividing it by the *TBP* expression level. RER of each target gene is defined as a quotient between treated and untreated samples, based on the absolute quantity levels, and is expressed in arbitrary units (RER = [absolute target gene $\text{quantity}_{\text{treated sample}}$ (absolute $\text{quantity}_{\text{target gene}}$/absolute quantity_{TBP})]/[absolute target gene $\text{quantity}_{\text{untreated sample}}$ (absolute $\text{quantity}_{\text{target gene}}$/absolute quantity_{TBP})]). As *shh* is a gene which is not expressed endogenously in the anterior section of the limb buds, RER for *shh* (RER_{shh}) was determined as a quotient between at-RA- and *S*-4o9cDH-RA-treated samples (RER_{shh} = [absolute *shh* $\text{quantity}_{\text{at-RA-treated sample}}$ (absolute quantity_{shh}/absolute quantity_{TBP})]/[absolute *shh* $\text{quantity}_{S\text{-4o9cDH-RA-treated sample}}$ (absolute quantity_{shh}/absolute quantity_{TBP})]). The reported data are the arithmetic mean ± SD for individual groups of different treatments. All statistical analysis was assessed using SIGMASTAT statistical software (Jandel Scientific, Erkath, Germany). When the data were normally distributed (Kolmogorov–Smirnov test), the paired *t*-test was used to test statistically significant differences between controls and treated samples. The level of significance was selected as $P < 0.05$. Group sizes are indicated in the table and figures.

Acknowledgements

The support of the European Union programmes BONETOX, NUTRICEPTORS and CASCADE is gratefully acknowledged. We thank all partners of these EU programmes for fruitful discussions and Malin Hedengran Faulds for provision of the HC11-RARE cell line.

References

1 Luo T, Sakai Y, Wagner E & Dräger UC (2006) Retinoids, eye development, and maturation of visual function. *J Neurobiol* **66**, 677–686.
2 Niederreither K & Dollé P (2008) Retinoic acid in development: towards an integrated view. *Nat Rev Genet* **9**, 541–553.
3 Duester G (2008) Retinoic acid synthesis and signaling during early organogenesis. *Cell* **134**, 921–931.

4 Campo-Paysaa F, Marlétaz F, Laudet V & Schubert M (2008) Retinoic acid signaling in development: tissue-specific functions and evolutionary origins. *Genesis* **46**, 640–656.
5 Kim CH (2008) Roles of retinoic acid in induction of immunity and immune tolerance. *Endocr Metab Immune Disord Drug Targets* **8**, 289–294.
6 Blomhoff R & Blomhoff HK (2006) Overview of retinoid metabolism and function. *J Neurobiol* **66**, 606–630.
7 Parés X, Farrés J, Kedishvili N & Duester G (2008) Medium- and short-chain dehydrogenase/reductase gene and protein families: medium-chain and short-chain dehydrogenases/reductases in retinoid metabolism. *Cell Mol Life Sci* **65**, 3936–3949.
8 Bastien J & Rochette-Egly C (2004) Nuclear retinoid receptors and the transcription of retinoid-target genes. *Gene* **328**, 1–16.
9 Mark M, Ghyselinck NB & Chambon P (2006) Function of retinoid nuclear receptors: lessons from genetic and pharmacological dissections of the retinoic acid signaling pathway during mouse embryogenesis. *Annu Rev Pharmacol Toxicol* **46**, 451–480.
10 Nuclear Receptors Nomenclature Committee (1999) A unified nomenclature system for the nuclear receptor superfamily. *Cell* **97**, 161–163.
11 de Lera AR, Bourguet W, Altucci L & Gronemeyer H (2007) Design of selective nuclear receptor modulators: RAR and RXR as a case study. *Nat Rev Drug Discov* **6**, 811–820.
12 Laudet V & Gronemeyer H (2002) *The Nuclear Receptor Factsbook*. *FactsBook Series*. Elsevier Academic Press, San Diego, CA.
13 Balmer JE & Blomhoff R (2002) Gene expression regulation by retinoic acid. *J Lipid Res* **43**, 1773–1808.
14 Tickle C (1991) Retinoic acid and chick limb bud development. *Dev Suppl* **1**, 113–121.
15 Tickle C, Alberts B, Wolpert L & Lee J (1982) Local application of retinoic acid to the limb bond mimics the action of the polarizing region. *Nature* **296**, 564–566.
16 Summerbell D (1983) The effect of local application of retinoic acid to the anterior margin of the developing chick limb. *J Embryol Exp Morphol* **78**, 269–289.
17 Tickle C, Lee J & Eichele G (1985) A quantitative analysis of the effect of all-*trans*-retinoic acid on the pattern of chick wing development. *Dev Biol* **109**, 82–95.
18 Francis PH, Richardson MK, Brickell PM & Tickle C (1994) Bone morphogenetic proteins and a signalling pathway that controls patterning in the developing chick limb. *Development* **120**, 209–218.
19 Izpisua-Belmonte JC & Duboule D (1992) Homeobox genes and pattern formation in the vertebrate limb. *Dev Biol* **152**, 26–36.
20 Charite J, de Graaff W, Shen S & Deschamps J (1994) Ectopic expression of Hoxb-8 causes duplication of the ZPA in the forelimb and homeotic transformation of axial structures. *Cell* **78**, 589–601.
21 Helms J, Thaller C & Eichele G (1994) Relationship between retinoic acid and sonic hedgehog, 2 polarizing signals in the chick wing bud. *Development* **120**, 3267–3274.
22 Hayamizu TF & Bryant SV (1994) Reciprocal changes in Hox D13 and RAR-beta 2 expression in response to retinoic acid in chick limb buds. *Dev Biol* **166**, 123–132.
23 Lu HC, Revelli JP, Goering L, Thaller C & Eichele G (1997) Retinoid signaling is required for the establishment of a ZPA and for the expression of Hoxb-8, a mediator of ZPA formation. *Development* **124**, 1643–1651.
24 Stratford TH, Kostakopoulou K & Maden M (1997) Hoxb-8 has a role in establishing early anterior–posterior polarity in chick forelimb but not hindlimb. *Development* **124**, 4225–4234.
25 Riddle RD, Johnson RL, Laufer E & Tabin C (1993) Sonic-hedgehog mediates the polarizing activity of the Zpa. *Cell* **75**, 1401–1416.
26 Duprez D, Lapointe F, Edom-Vovard F, Kostakopoulou K & Robson L (1999) Sonic hedgehog (SHH) specifies muscle pattern at tissue and cellular chick level, in the chick limb bud. *Mech Dev* **82**, 151–163.
27 Swindell EC, Thaller C, Sockanathan S, Petkovich M, Jessell TM & Eichele G (1999) Complementary domains of retinoic acid production and degradation in the early chick embryo. *Dev Biol* **216**, 282–296.
28 Martinez-Ceballos E & Burdsal CA (2001) Differential expression of chicken CYP26 in anterior versus posterior limb bud in response to retinoic acid. *J Exp Zool* **290**, 136–147.
29 Abu-Abed S, Dollé P, Metzger D, Beckett B, Chambon P & Petkovich M (2001) The retinoic acid-metabolizing enzyme, CYP26A1, is essential for normal hindbrain patterning, vertebral identity, and development of posterior structures. *Genes Dev* **15**, 226–240.
30 Yashiro K, Zhao X, Uehara M, Yamashita K, Nishijima M, Nishino J, Saijoh Y, Sakai Y & Hamada H (2004) Regulation of retinoic acid distribution is required for proximodistal patterning and outgrowth of the developing limb. *Dev Cell* **6**, 411–422.
31 Uehara M, Yashiro K, Mamiya S, Nishino J, Chambon P, Dolle P & Sakai Y (2007) CYP26A1 and CYP26C1 cooperatively regulate anterior–posterior patterning of the developing brain and the production of migratory cranial neural crest cells in the mouse. *Dev Biol* **302**, 399–411.
32 Schmidt CK, Volland J, Hamscher G & Nau H (2002) Characterization of a new endogenous vitamin A metabolite. *Biochim Biophys Acta* **1583**, 237–251.
33 Heyman RA, Mangelsdorf DJ, Dyck JA, Stein RB, Eichele G, Evans RM & Thaller C (1992) 9-*cis* retinoic

acid is a high affinity ligand for the retinoid X receptor. *Cell* **68**, 397–406.
34 Pijnappel WW, Folkers GE, de Jonge WJ, Verdegem PJ, de Laat SW, Lugtenburg J, Hendriks HF, van der Saag PT & Durston AJ (1998) Metabolism to a response pathway selective retinoid ligand during axial pattern formation. *Proc Natl Acad Sci USA* **95**, 15424–15429.
35 Tzimas G, Sass JO, Wittfoht W, Elmazar MM, Ehlers K & Nau H (1994) Identification of 9,13-dicis-retinoic acid as a major plasma metabolite of 9-*cis*-retinoic acid and limited transfer of 9-*cis*-retinoic acid and 9,13-dicis-retinoic acid to the mouse and rat embryos. *Drug Metab Dispos* **22**, 928–936.
36 Shirley MA, Bennani YL, Boehm MF, Breau AP, Pathirana C & Ulm EH (1996) Oxidative and reductive metabolism of 9-*cis*-retinoic acid in the rat. Identification of 13,14-dihydro-9-*cis*-retinoic acid and its taurine conjugate. *Drug Metab Dispos* **24**, 293–302.
37 Levin AA, Sturzenbecker LJ, Kazmer S, Bosakowski T, Huselton C, Allenby G, Speck J, Kratzeisen C, Rosenberger M, Lovey A *et al.* (1992) 9-*cis* retinoic acid stereoisomer binds and activates the nuclear receptor RXR alpha. *Nature* **355**, 359–361.
38 Allenby G, Bocquel M-T, Saunders M, Kazmer S, Speck J, Rosenberger M, Lovey A, Kastner P, Grippo JF, Chambon P *et al.* (1993) Retinoic acid receptors and retinoid X receptors: interactions with endogenous retinoic acids. *Proc Natl Acad Sci USA* **90**, 30–34.
39 Zhang X, Lehmann J, Hoffmann B, Dawson MI, Cameron J, Graupner G, Hermann T, Tran P & Pfahl M (1992) Homodimer formation of retinoid X receptor induced by 9-*cis* retinoic acid. *Nature* **358**, 587–591.
40 Kurokawa R, DiRenzo J, Boehm M, Sugarman J, Gloss B, Rosenfeld MG, Heyman RA & Glass CK (1994) Regulation of retinoid signalling by receptor polarity and allosteric control of ligand binding. *Nature* **371**, 528–531.
41 Germain P, Iyer J, Zechel C & Gronemeyer H (2002) Co-regulator recruitment and the mechanism of retinoic acid receptor synergy. *Nature* **415**, 187–192.
42 Mic FA, Molotkov A, Benbrook DM & Duester G (2003) Retinoid activation of retinoic acid receptor but not retinoid X receptor is sufficient to rescue lethal defect in retinoic acid synthesis. *Proc Natl Acad Sci USA* **100**, 7135–7140.
43 Calléja C, Messaddeq N, Chapellier B, Yang H, Krezel W, Li M, Metzger D, Mascrez B, Ohta K, Kagechika H *et al.* (2006) Genetic and pharmacological evidence that a retinoic acid cannot be the RXR-activating ligand in mouse epidermis keratinocytes. *Genes Dev* **20**, 1525–1538.
44 Zelent A, Krust A, Petkovich M, Kastner P & Chambon P (1989) Cloning of murine alpha and beta retinoic acid receptors and a novel receptor gamma predominantly expressed in skin. *Nature* **339**, 714–717.
45 Moise AR, Kuksa V, Blaner WS, Baehr W & Palczewski K (2005) Metabolism and transactivation activity of 13,14-dihydroretinoic acid. *J Biol Chem* **280**, 27815–27825.
46 Pijnappel WWM, Hendriks HFJ, Folkers GE, Vandenbrink CE, Dekker EJ, Edelenbosch C, van der Saag PT & Durston AJ (1993) The retinoid ligand 4-oxo-retinoic acid is a highly-active modulator of positional specification. *Nature* **366**, 340–344.
47 Reynolds NJ, Fisher GJ, Griffiths CEM, Tavakkol A, Talwar HS, Rowse PE, Hamilton TA & Voorhees JJ (1993) Retinoic acid metabolites exhibit biological-activity in human keratinocytes, mouse melanoma-cells and hairless mouse skin in-vivo. *J Pharmacol Exp Ther* **266**, 1636–1642.
48 Nikawa T, Schulz WA, van den Brink CE, Hanusch M, van der Saag P, Stahl W & Sies H (1995) Efficacy of all-*trans*-beta-carotene, canthaxanthin, and all-*trans*-, 9-*cis*-, and 4-oxoretinoic acids in inducing differentiation of an F9 embryonal carcinoma RAR beta-lacZ reporter cell line. *Arch Biochem Biophys* **316**, 665–672.
49 van der Leede BM, van den Brink CE, Pijnappel WW, Sonneveld E, van der Saag PT & van der Burg B (1997) Autoinduction of retinoic acid metabolism to polar derivatives with decreased biological activity in retinoic acid-sensitive, but not in retinoic acid-resistant human breast cancer cells. *J Biol Chem* **272**, 17921–17928.
50 Niederreither K, Abu-Abed S, Schuhbaur B, Petkovich M, Chambon P & Dollé P (2002) Genetic evidence that oxidative derivatives of retinoic acid are not involved in retinoid signaling during mouse development. *Nat Genet* **31**, 84–88.
51 Ruiz A, Winston A, Lim YH, Gilbert BA, Rando RR & Bok D (1999) Molecular and biochemical characterization of lecithin retinol acyltransferase. *J Biol Chem* **274**, 3834–38341.
52 Moise AR, Kuksa V, Imanishi Y & Palczewski K (2004) Identification of all-*trans*-retinol:all-*trans*-13,14-dihydroretinol saturase. *J Biol Chem* **279**, 50230–50242.
53 Arnhold T, Tzimas G, Wittfoht W, Plonait S & Nau H (1996) Identification of 9-*cis*-retinoic acid, 9,13-di-*cis*-retinoic acid, and 14-hydroxy-4,14-retro-retinol in human plasma after liver consumption. *Life Sci* **59**, PL169–PL177.
54 Urbach J & Rando RR (1994) Isomerization of all-*trans*-retinoic acid to 9-*cis*-retinoic acid. *Biochem J* **299**, 459–465.
55 Thaller C & Eichele G (1990) Isolation of 3,4-didehydroretinoic acid, a novel morphogenetic signal in the chick wing bud. *Nature* **345**, 815–819.
56 Thaller C, Hofmann C & Eichele G (1993) 9-*cis*-retinoic acid, a potent inducer of digit pattern duplications in the chick wing bud. *Development* **118**, 957–965.

57 Loudig O, Babichuk C, White J, Abu-Abed S, Mueller C & Petkovich M (2000) Cytochrome P450RAI(CYP26) promoter: a distinct composite retinoic acid response element underlies the complex regulation of retinoic acid metabolism. *Mol Endocrinol* **14**, 1483–1497.

58 Oosterveen T, Niederreither K, Dolle P, Chambon P, Meijlink F & Deschamps J (2003) Retinoids regulate the anterior expression boundaries of 5′ Hoxb genes in posterior hindbrain. *EMBO J* **22**, 262–269.

59 Sucov HM, Murakami KK & Evans RM (1990) Characterization of an autoregulated response element in the mouse retinoic acid receptor type beta gene. *Proc Natl Acad Sci USA* **87**, 5392–5396.

60 de The H, Vivanco-Ruiz MM, Tiollais P, Stunnenberg H & Dejean A (1990) Identification of a retinoic acid responsive element in the retinoic acid receptor beta gene. *Nature* **343**, 177–180.

61 Schmidt CK, Brouwer A & Nau H (2003) Chromatographic analysis of endogenous retinoids in tissues and serum. *Anal Biochem* **315**, 36–48.

62 Pozzi S, Rossetti S, Bistulfi G & Sacchi N (2006) RAR-mediated epigenetic control of the cytochrome P450 Cyp26a1 in embryocarcinoma cells. *Oncogene* **25**, 1400–1407.

63 Hamburger V & Hamilton HL (1951) A series of normal stages in the development of the chick embryo. *J Morphol* **88**, 49–67.